Toward Single-Cycle Biphotons

Stephen E. Harris and Steven Sensarn
Ginzton Laboratory, Stanford University, Stanford, California, 94305
seharris@stanford.edu

Abstract: The paper describes a technique for the spontaneous generation of chirped biphotons and for the compression of these photons to transform limited biphotons. At maximum bandwidth the biphoton is a single-cycle in length and has the waveform of a classical single-cycle pulse. Without compression, chirped biphotons still exhibit a Hong-Ou-Mandel dip with a width approximately equal to the inverse spectral width of the biphoton.

OCIS codes: 030.1640, 270.4180, 320.1590

1. Introduction

It is the intent of this paper to explore the interplay of some of the concepts of ultra-short time scale laser physics with the concepts of quantum optics. We are interested in the possibility of generating time-energy entangled photons with a spectrum that approaches or exceeds an octave in width, and of compressing this spectrum so as to produce biphotons whose temporal length is, ultimately, a single optical cycle [1]. The elements of the technique are: (1) the suggestion for using parametric down conversion in a periodically poled material to spontaneously generate pairs of entangled photons whose instantaneous frequencies are chirped in opposite directions, and (2) the use of the non-local nature of entangled photons to allow the dispersion, as experienced by one photon, to cancel out the dispersion of the second photon and to compress the biphoton wave packet. Technologically, we make use of the science and art of periodic poling of nonlinear optical crystals [2].

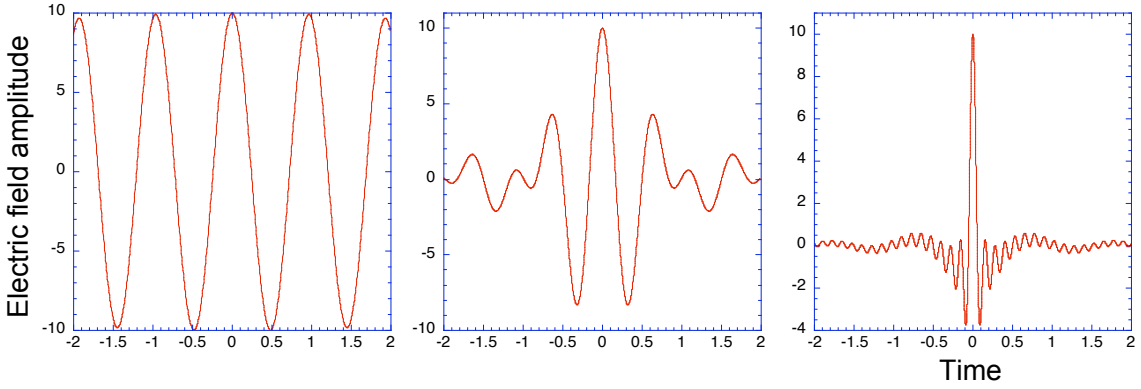

Fig. 1. Optical waveform as a function of bandwidth. Each portion of this figure shows the optical waveform obtained by summing one hundred equally spaced modes which have the same amplitude and phase. The variable is the number of octaves ζ spanned by these modes. From left to right, $\zeta = 0.1$, $\zeta = 1$, and $\zeta = 3$, respectively.

Figure 1 shows the electric field amplitude obtained by summing one hundred and one equally spaced optical modes, all with the same amplitude and the same phase; i.e. $E(t) = \Re \sum_{n=0}^{100} a_n \exp[i(f_0 + nf_v)t]$ where the modes span the frequency interval from $f_0 = 1$ to f_{max}, and the number of octaves $\zeta = \log_2(f_{max}/f_0)$. If the number of octaves is small, for example 0.1, then the wave form is nearly sinusoidal. At one octave of bandwidth, the waveform begins to develop the characteristic shape of what is termed as a single-cycle optical pulse. For three or more octaves of

bandwidth, the shape is nominally invariant to further increases in bandwidth. The special feature of this waveform is the appearance of a pseudo-polarity, with a sign determined by the carrier envelope phase. The properties and propagation of single-cycle optical pulses have been discussed by You and Bucksbaum [3]. The observation of a train of optical pulses where each pulse is approximately a single cycle in length has been reported by Shverdin, et al. [4].

A motivation for the study of single-cycle biphotons is their potential application to nonlinear optical processes with nonclassical fields [5]. Following the experiments of Silberberg [6], and the calculations of Dowling [7] we will use sum frequency generation as an ultra-fast correlator. As will be discussed further below, the efficiency for generating sum frequency photons varies inversely with temporal width of the incoming biphoton; i.e. single cycle biphotons behave as if they have an effective power equal to their energy divided by their temporal width. In the absence of intermediate resonances, single-cycle biphotons also maximize two photon transition probabilities. Other uses for ultra-wideband biphotons might include non-classical metrology [8] and large bandwidth quantum information processing [9] using both Franson and Hong-Ou-Mandel interferometers [10].

We note the early suggestion of Torner and Teich et al. [11] for using chirped quasi-phase-matched nonlinear crystals to broaden the emission bandwidth of spontaneous parametric down conversion. First experimental results are reported at this meeting by Nasr and colleagues (paper IThH5) [12].

2. Chirped Biphotons

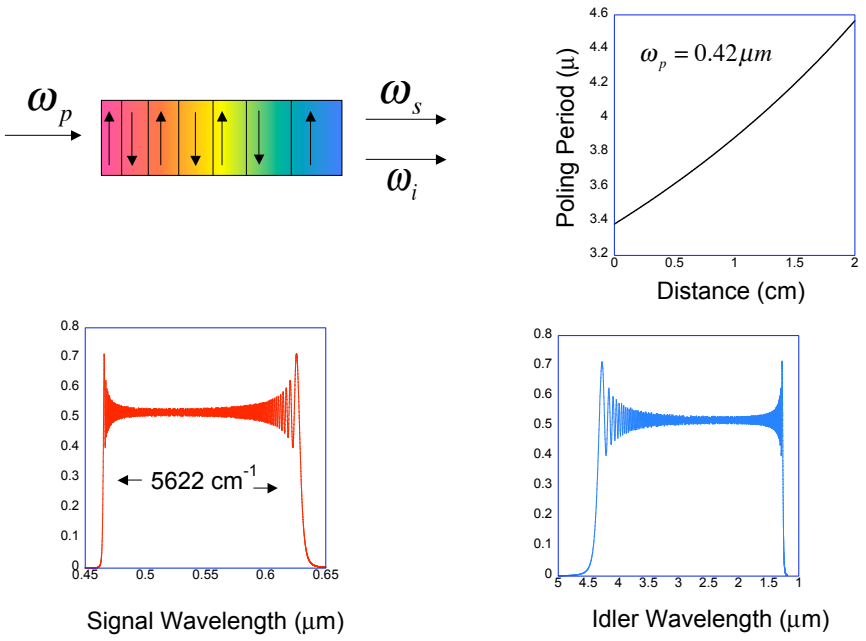

Fig. 2. Spectrum of spontaneously generated photons for a 2 cm long QPM crystal of $LiNbO_3$ pumped at 0.42 μ. We assume that the periodic poling is apodized to remove the frequency dependence of the coupling constant so as to produce a flat spectrum. Reprinted from Ref [1].

Figure 2 shows the spontaneously emitted spectrum when the spatial frequency of the poling function is linearly chirped. The spatial frequency of the domain reversals varies linearly with distance and is chosen so that the crystal is phase matched at a signal wavelength of 0.750 μm at the left edge and at a wavelength of 0.464 μm at the right edge. Paired photons that are emitted from the right edge of the crystal arrive at photodetectors at the same time. Paired photons that are emitted from the left edge of the crystal arrive at the photodetector with a time difference set by

their respective group velocities. In the ideal case where there is no group velocity dispersion the biphoton is linearly chirped. For a red-to-blue chirped crystal that is 2 cm long, the difference in arrival time between a red photon and its corresponding idler photon, both emitted from the left hand edge of the crystal, is about 20 ps. When compressed this spectrum corresponds to a biphoton with a temporal length that is nearly a single optical cycle at the degenerate wavelength of 0.84 μm. (The refractive index as a function of frequency is $n_e(\omega)$ and is obtained from the Sellmeier equation for $\bar{a}_z$ polarized light in $LiNbO_3$). The essential point is that by chirping the k-vector of the periodic poling function, we localize the position in the crystal at which a particular signal-idler pair is emitted. Position becomes time delay, and time delay (as a function of frequency) may then be corrected with a dispersive element.

We take the spatial frequency of the QPM crystal as $K_0 - \zeta z$ where K_0 is chosen to phase match the crystal at a selected frequency at its left end, and ζ is chosen to phase match a selected frequency at its right end . The functional form of the spatially varying nonlinearity is then $\exp(i\int_0^z \zeta z dz) = \exp(i\zeta z^2/2)$. With V_s and V_i defined as the group velocities at the signal and the idler, and $1/V_r = |1/V_s - 1/V_i|$, then in the absence of group velocity dispersion, the bandwidth of the generated signal and idler photons for a crystal of length L is $\zeta V_r L$. The total paired count rate is independent of the chirping parameter ζ. For the 2 cm crystal of $LiNbO_3$ pumped by a confocally focused 1 W laser at 0.42 μm, the integrated count rate for the spectrum of Fig (2) is calculated as 1.3×10^{10} pairs s^{-1}.

2.1. Analysis

We assume a monochromatic pump at ω_p, and take the signal and idler frequencies as $\omega_s = \omega$, and $\omega_i = \omega_p - \omega$. Both the signal and idler frequencies are positive with the signal frequency defined to be in the range $\omega_p/2 \leq \omega \leq \omega_p$. Time domain signal and idler operators are related to their frequency domain counterparts by $a_s(t,z) = \int_{-\infty}^{\infty} a_s(\omega,z)\exp(-i\omega t)d\omega$ and $a_i(t,z) = \int_{-\infty}^{\infty} a_i(\omega_i,z)\exp[-i(\omega_p-\omega)t]\,d\omega$. We introduce operators $b(\omega,z)$ that vary slowly with distance, as compared to a wavelength, by letting $a(\omega,z) = b(\omega,z)\exp[ik(\omega)z]$. The coupled equations for the operators $b_s(\omega_s,z)$ and $b_i^\dagger(\omega_i,z)$ are

$$\begin{aligned}\frac{\partial b_s}{\partial z} &= i\kappa b_i^\dagger \exp\left(i\frac{\zeta z^2}{2}\right)\exp[i\Delta k(\omega)z]\\ \frac{\partial b_i^\dagger}{\partial z} &= -i\kappa^* b_s \exp\left(-i\frac{\zeta z^2}{2}\right)\exp[-i\Delta k(\omega)z].\end{aligned} \tag{1}$$

The quantity $\Delta k(\omega) = k_p(\omega_p) - [k_s(\omega) + k_i(\omega_i) + K_0]$, where $k(\omega) = \omega n(\omega)/c$. Dispersion, to all orders, is included in Eq.(1), and there is no assumption requiring that the temporal variation be slow.

Working in the Heisenberg picture, and following Ref [1], the signal and idler operators $a_s(\omega,L)$, and $a_i^\dagger(\omega_i,L)$ at the output of a crystal of length L, may be written as

$$\begin{aligned}a_s(\omega,L) &= A_1(\omega)\,a_s(\omega,0) + B_1(\omega)\,a_i^\dagger(\omega_i,0)\\ a_i^\dagger(\omega_i,L) &= C_1(\omega)\,a_s(\omega,0) + D_1(\omega)\,a_i^\dagger(\omega_i,0)\end{aligned} \tag{2}$$

where $A_1(\omega) = \exp[ik_s(\omega)L]$, $D_1(\omega) = \exp[-ik_i(\omega_i)L]$, $C_1(\omega) = B_1^*(\omega)\exp[i\,(k_s(\omega) - k_i(\omega_i))\,L]$, and

$$\begin{aligned}B_1(\omega) = &-(-1)^{\frac{1}{4}}\left(\frac{\pi}{2}\right)^{\frac{1}{2}}\frac{1}{\sqrt{\zeta}}\kappa\exp[ik_s(\omega)L]\exp[\tfrac{-i\Delta k(\omega)^2}{2\zeta}]\\ &\times\left\{\text{erfi}\left[\tfrac{(1+\text{i})\Delta\text{k}(\omega)}{2\sqrt{\zeta}}\right] - \text{erfi}\left[\tfrac{(1+\text{i})(\Delta\text{k}(\omega)+\zeta\text{L})}{2\sqrt{\zeta}}\right]\right\}.\end{aligned} \tag{3}$$

The commutator $[a_j(\omega_1,0), a_k^\dagger(\omega_2,0)] = \frac{1}{2\pi}\delta_{jk}\delta(\omega_1-\omega_2)$, and erfi is the imaginary error function. (The expression for $B_1(\omega)$, as above, corrects a sign error in Ref [1] that occurs when ζ is negative.) From the functional form of $B_1(\omega)$, we deduce that to attain bandwidth limited compression of the chirped biphoton we should place an optical element in the path of the signal beam whose transfer function is

$$H(\omega) = \exp\left[i\left(\frac{\Delta k(\omega)^2}{2\zeta} - q(\omega)\right)\right] \tag{4}$$

where $q(\omega) = [k_s(\omega) + k_i(\omega_p - \omega)]\,L$. The effect of this transfer function is to cause the paired signal and idler photons, irrespective of their frequencies, to arrive at distant detectors (or at the summing crystal) at the same time. Though neither the signal or the idler photon is itself transform limited, the biphoton is.

3. Mandel Dip

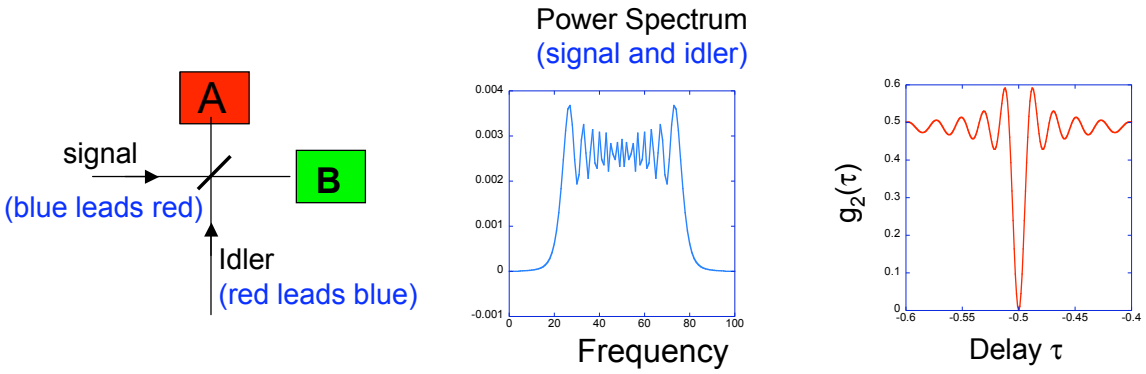

Fig. 3. Mandel dip with chirped biphotons. Here, the signal and idler have the same spectral power density and are chirped in the opposite sense. The Mandel dip has a width equal to the inverse of its spectral width, and occurs at the mid-point of the chirped biphoton.

We have shown analytically that chirped biphotons, if ideal, and with a detector that is slow as compared to the width of the biphoton, will allow a perfect Hong-Ou-Mandel dip without temporal compensation. This may be viewed as a corollary to the well known Steinberg-Kwiat-Chiao prediction of the immunity of Mandel dip to group velocity dispersion [13]. Figure 5 shows the normalized Glauber correlation function for a hypothetical, ideal case where the signal and idler photons have the same power spectrum, but where the signal frequency is chirped from blue toward red and the idler frequency is chirped from red toward blue. We assume a group velocity that is independent of frequency (no GVD). For this example, the chirped biphoton has a temporal width of one unit, and a spectral width of 100 units. The dip occurs at the mid-point of the chirped biphoton with a temporal width that is equal to the inverse of its spectral width.

If one attempts to attain Mandel dips with very wide bandwidths, then it will be necessary to compensate for higher odd order dispersive terms. This may be done with appropriate changes in the periodic poling function. Though in this work we describe chirped biphotons using a cw pumping source, extension to a pulsed pump, as described by Walmsley and colleagues, seem likely [14].

A first experiment showing a Mandel Dip using chirped periodic poling is reported at this meeting by Nasr and colleagues (paper IThH5) [12].

4. Biphoton Correlation and Waveform

We are interested in compressing biphotons to times on order of a single optical cycle, and therefore much shorter than the response time of avalanche photo diodes. We follow Silberberg [6] and make use of sum frequency generation as an ultra-fast correlator. Because the phase of the biphoton plays a role in what follows we will homodyne the generated sum frequency against the original pumping beam. A schematic of the experiment that we plan to construct is shown in Fig. 4. In Fig. 4 (a), the signal and idler photons sum to generate monochromatic photons at the pump frequency ω_p. Because the signal and idler photons arrive at the second nonlinear crystal simultaneously, the rate of generated sum frequency photons varies linearly (rather than as the square) of the rate of incoming paired photons. By measuring the average power at the sum frequency as a function of the time delay τ between the signal and idler photons, we measure the correlation function $g^2(\tau)$. In a summing experiment of this type, but near degeneracy [6], Silberberg and colleagues report an estimated count rate at the sum frequency of 40,000 counts per second. Here, because the bandwidths will be much broader, to allow phase matching, the summing crystal must be very thin, and we anticipate about 100 counts per second. To measure the waveform, rather than its envelope, we require a reference phase. As shown in Fig. 4 (b) we obtain this phase by homodyning the generated sum frequency against the original monochromatic pumping laser, and as before, varying the path length of the idler beam τ.

To write the expression for the generated sum power we replace the coefficients in Eq. (2) with coefficients that

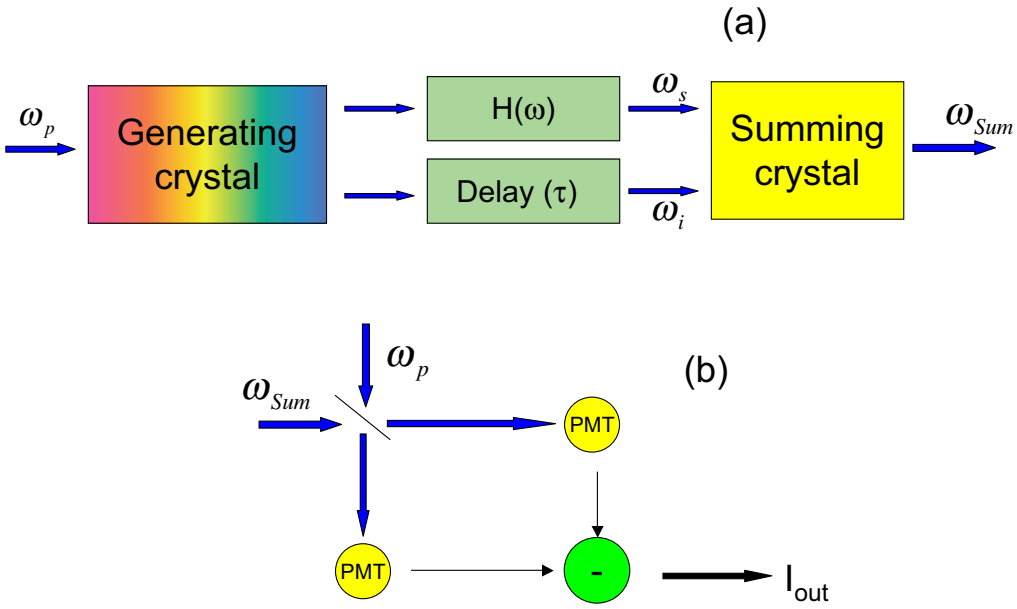

Fig. 4. (a) Frequency Summing as an ultrafast correlator. Signal and idler photons sum to produce monochromatic photons at frequency ω_p. The envelope of the biphoton wavefunction is obtained by varying the time delay τ. (b) Homodyning the generated sum frequency with the pump beam, and varying the time delay τ yields the biphoton wavefunction.

include the dispersion compensating function $H(\omega)$ in the signal channel, and a time delay function $G(\omega,\tau) = \exp[-i(\omega_p-\omega)\tau]$ in the idler channel . These are: $A(\omega)$=$H(\omega)A_1(\omega)$, $B(\omega) = H(\omega)B_1(\omega)$, $C(\omega,\tau) = G(\omega,\tau)C_1(\omega)$, and $D(\omega,\tau) = G(\omega,\tau)D_1(\omega)$.

The rate of generated sum photons is then [1]

$$R_{sum}(\tau) = \eta_1 \left[R^2 + \left| \left(\frac{1}{2\pi}\right) \int_{\omega_p/2}^{\omega_p} A(\omega)C^*(\omega,\tau)d\omega \right|^2 \right]. \tag{5}$$

The first term in Eq. (4) is the same as its classical equivalent where the output power depends on the square of the input power, and the efficiency factor η_1 is equal to its classical value. The second term is equal to the square of the amplitude of the biphoton wavefunction. For a wave function of width T_p, the ratio of the peak height of the second term as compared to the first term is approximately $1/(RT_p)$.

The output current of the balanced homodyne detector is calculated as

$$I_{out} = \left(\frac{1}{2\pi}\right) \Re \left[\int_{\omega_p/2}^{\omega_p} e^{i\phi} A(\omega)C^*(\omega)d\omega \right] \tag{6}$$

Here, ϕ is the phase of the local oscillator with respect to the pumping beam.

4.1. Compression of a Chirped Pulse

The compression of the chirped pulse is possible due to the nonlocal nature of entangled photons that allows the dispersion, as experienced by one photon, to cancel out the dispersion of the second photon and to compress the biphoton wavepacket. Classically, this is not possible; and broadening of either pulse may not be cancelled by compression of the other [15].

Figure 5 shows an example of the chirp and compress technique for $LiNbO_3$ with a small chirp and quadratic compression. For comparison, Fig. 5(a) shows sum power, normalized to the classically generated power, for a uniformly poled (non-chirped) crystal of length of 2 cm and relative group velocity V_r. The width of the envelope of the biphoton wave function is L/V_r [16] and is 12.6 ps, and the linewidth is 2.6 cm^{-1}. For Fig. 5(b), the poling period

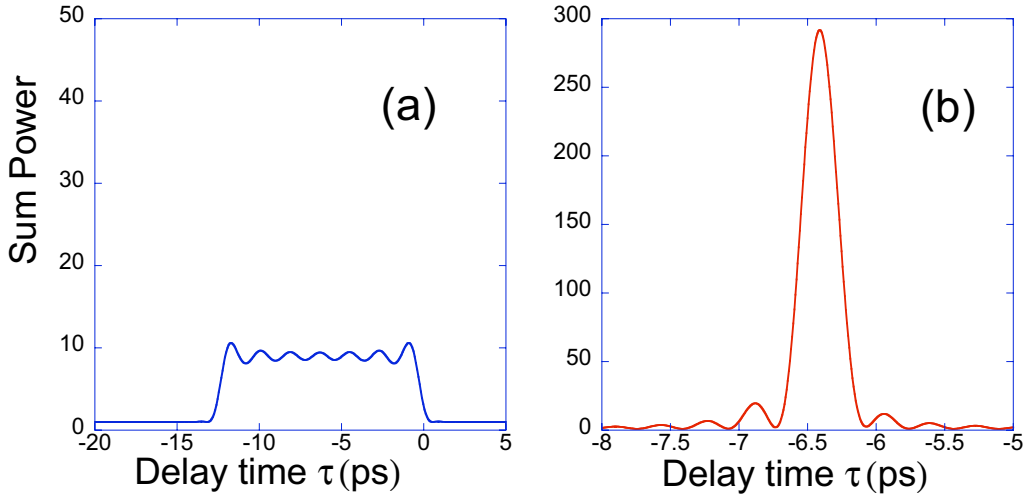

Fig. 5. Calculated normalized sum power as a function of delay. (a) The QPM crystal is uniformly poled to phase match at 0.6 μm with a bandwidth of 2.6 cm^{-1}. (b) The poling period is chirped to produce a bandwidth of 122 cm^{-1} and the wavepacket is quadratically compressed.

is chirped with parameter $\zeta = 6.01 \times 10^5$ to produce a bandwidth of 122 cm^{-1}. A compressor with transfer function $H(\omega) = \exp[i\delta\omega^2/(2V_r{}^2\zeta)]$ is used [1]. The width of the biphoton wavepacket is reduced and the sum power is increased, both by a factor of about thirty.

4.2. Carrier-Envelope Phase

The term carrier-envelope phase, as used in ultrafast optics, denotes the phase difference between the peak of an ultrashort pulse's envelope and the closest peak of the carrier wave on which it is superimposed. In quantum optics, the Glauber correlation function $g^{(2)}(\tau)$ as obtained by measuring the sum frequency power as a function of the delay τ yields the envelope of the biphoton wave function. To obtain the waveform itself we homodyne the generated monochromatic sum frequency against the pump. As shown in Fig. 6, the polarity and shape of the single-cycle waveform depend on the relative phase between the pump and the sum frequency radiation. The waveform at a relative phase $\phi = \pi/2$ is the negative of the derivative of the waveform at $\phi = 0$, and could instead be obtained by propagating the signal and idler beams from the near-field to the far-field before summing [17]. From the experiments of Mandel and colleagues it is understood that down-converted photons carry information about the phase of the pump field [18]. Here, that phase information manifests as the carrier-envelope phase of ultrafast optics.

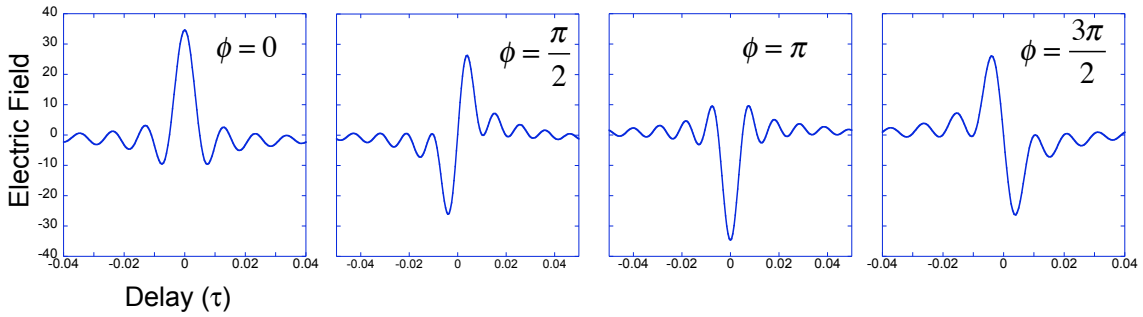

Fig. 6. Homodyne output current as a function of the delay τ with variable carrier envelope phase ϕ.

5. Acknowledgements

The work described here has been supported by the U.S. Air Force Office of Scientific Research, the U.S. Army Research Office, and the Defense Advanced Research Projects Agency. The authors acknowledge helpful discussions with Pavel Kolchin, Irfan Ali Khan and Paul Kwiat.

References

1. S. E. Harris, Phys. Rev. Lett. **98**, 063602 (2007).
2. L. E. Myers, R. C. Eckardt, M. M. Fejer, and R. L. Byer, J. Opt. Soc. Am. B **12**, 210 (1995).
3. D. You and P. H. Bucksbaum, J. Opt. Soc. Am. B **14**, 1651 (1997).
4. M. Y. Shverdin, D. R. Walker, D. D. Yavuz, G. Y. Yin, and S. E. Harris, Phys. Rev. Lett. **94**, 033904 (2005).
5. J. Gea-Banacloche, Phys. Rev. Lett., **62**,1603,1989; N. Ph. Georgiades, E. S. Polzik, K. Edamatsu, H. J. Kimble, A.S. Parkins, Phys. Rev. Lett. **75**, 3426 (1995).
6. B. Dayan, A. Pe'er, A. Friesem, and Y. Silberberg, Phys. Rev. Lett. **94**, 043602 (2005).
7. D.V. Streklov, M.C. Stowe, M.V. Chekjova, and J.P. Dowling, Journal of Modern Optics. **49** , 2349, (2002).
8. V. Giovannetti, S Lloyd, L Maccone, Phys. Rev. Lett. **96**, 010401 (January 2006).
9. C. K. Law, I. A. Walmsley, and J. H. Eberly, Phys. Rev. Lett. **84**, 5304 (2000).
10. I. A. Khan and J.C. Howell, Phys. Rev. A, **73**, 031801(R) (2006).
11. S. Carrasco, J. P. Torres, and L. Torner, A. Sergienko, B. Saleh, M. Teich, Opt. Lett. **29**, 2429 (2004).
12. M. B. Nasr, et al., Proceedings of CQO9, (2007).
13. A.M. Steinberg, P.G. Kwiat, and R.Y.Chiao, Phys. Rev. A, **45**, 6659 (1992).
14. R. Erdmann, D. Branning, W. Grice, I.A. Walmsley, Phys. Rev. A, **62**, 053810 (2000).
15. J. D. Franson, Phys. Rev. A, **45**, 3126 (1992).
16. M. H. Rubin, D.N. Klyshko, Y.H. Shih, and A.V. Sergienko, Phys. Rev. A, **50**, 5122 (1994).
17. S. E. Harris, J. J. Macklin, and T. W. Hänsch, Opt. Commun. **100**, 487 (1993).
18. Z. Y. Ou, L. J. Wang, X. Y. Zou, and L. Mandel, Phys. Rev. A **41**, 566 (1990).